Catalysis Today 136 (2008) 266–272

Contents lists available at ScienceDirect

Catalysis Today

journal homepage: www.elsevier.com/locate/cattod

Production of synthesis gas by autothermal reforming of *iso*-octane and toluene over metal modified Ni-based catalyst

Dae Hyun Kim, Jong Woo Ryu, Eun Hyung Choi, Gyeong Taek Gong, Hyunjoo Lee, Byung Gwon Lee, Dong Ju Moon *

Clean Energy Research Center, Korea Institute of Science and Technology (KIST), P.O. Box 131, Cheongrayang, Seoul 130-650, Republic of Korea

ARTICLE INFO

Keywords:
ATR
iso-Octane
Gasoline fuel processor
Ni-based catalyst
Syngas production
Hydrogen station

ABSTRACT

The reforming process of gasoline is an attractive technique for fuel processor or hydrogen station applications. We investigated catalytic autothermal reforming (ATR) of *iso*-octane and toluene over transition metal supported catalysts. The catalysts were prepared by an incipient wetness impregnation method and characterized by N_2 physisorption, XRD, and TEM techniques before and after the reaction. Many of the tested catalysts displayed reasonably good activity towards the reforming reactions of *iso*-octane. Especially, $Ni/Fe/MgO/Al_2O_3$ catalyst showed more activity than the other catalysts tested in this study including commercial HT catalyst. $Ni/Fe/MgO/Al_2O_3$ catalyst showed good stability for 700 h in the ATR of *iso*-octane. No major change was observed in catalytic activity in ATR of *iso*-octane or in the structure of catalyst. Since *iso*-octane, toluene are surrogates of gasoline, $Ni/Fe/MgO/Al_2O_3$ catalyst can be considered as ATR catalyst for gasoline fuel processor and hydrogen station systems.

1. Introduction

Catalytic reforming of gasoline for producing hydrogen is an attractive option for use in the production of clean energy from proton exchanged membrane fuel cells (PEMFCs) and solid oxide fuel cell (SOFC) system. For autothermal reforming (ATR), built up of the centralized larger system can offer the ability to sequester CO_2 and scrub sulfur without significant increase in cost and benefiting reduction in pollution. The successful development of gasoline reformer for fuel processor or hydrogen station applications is dependent on the development of high performance catalysts.

Hydrogen is the ideal fuel for a PEM fuel cell because it simplifies the system integration. However, since no hydrogen fuel supply infrastructure currently exists, the development of fuel processor using LNG, LPG, methanol and gasoline is important. Regarding the existing reforming processes to generate hydrogen rich-gas, methanol yields the highest efficiency among all the available liquid fuels. However, the lower efficiency of gasoline in comparison with methanol can be compensated by the much higher energy density of gasoline compared to methanol and also by the well-developed infrastructure for gasoline [1]. Gasoline is recommended as the best candidate fuel for the fuel processor and hydrogen station.

Major process technologies for reforming hydrocarbons into hydrogen are catalytic steam reforming (SR), partial oxidation (POX) and autothermal reforming [2]. Steam-reforming reaction of hydrocarbons usually taking place at temperature around 700 °C seems to show the highest reforming efficiency. But the drawback is that this reaction is endothermic and therefore, the reactor needs to be heated by combustion of fuels itself. So far, no sulfur tolerant steam-reforming catalyst has been reported, resulting in the need for a very efficient and therefore, probably large unit for removing the sulfur contained in fuels [3–7,14]. POX and ATR systems do not require external heating like steam-reforming system and can be heated up internally relatively quickly by exothermic reaction of fuels. Hence, they are much dynamic than a steam-reforming system. The sulfur tolerance for ATR system is also better than that of steam reforming. Considering the favorable factors required for the production of hydrogen for application in stationary fuel cell system, the ATR process attracts much attention primarily due to the low energy requirement, the opposite contribution of the exothermic hydrocarbon oxidation and endothermic steam reforming, and also due to the high space velocity compared to the POX process [8].

Nickel-based catalysts are attractive for POX and ATR reactions due to their low cost, but Ni is easily deactivated by coke formation and/or by sintering. It is reported [9] that the addition of ZrO_2 to ceria leads to improvements in redox property, thermal resistance and better catalytic activity for ATR at lower temperatures.

* Corresponding author. Tel.: +82 2 958 5867.
E-mail address: djmoon@kist.re.kr (D.J. Moon).

0920-5861/$ – see front matter © 2008 Elsevier B.V. All rights reserved.
doi:10.1016/j.cattod.2008.02.021

In this work, ATR reaction of *iso*-octane and toluene over various transition metal formulations was investigated to develop a high performance catalyst with high activity and stability. Also the catalytic performance of prepared catalyst was compared with that of the commercial catalyst (Haldor Topsoe, HT).

2. Experimental

2.1. Chemicals

The *iso*-octane and toluene used as fuel sources were supplied by J.T. Baker. Hydrogen (99.999%), air (99.999%) and nitrogen (99.999%) were used in the reaction and also for the pretreatment of the catalysts. Nickel nitrate, cobalt nitrate, magnesium nitrate, ferric nitrate, ammonium molybdate and zirconyl oxynitrate hydrate were procured from Aldrich Chemicals and cerium(III) nitrate hexahydrate was procured from Acros Organics. Also, γ-alumina (2-3 microns) and urea (99.0%) were supplied by High Purity Chemicals and Fluka respectively.

2.2. Preparation of catalysts

$M_{(active)}/MgO/Al_2O_3$, $M_{(active)}/MgO/SiO_2$-Al_2O_3, $Ni_{(major)}/M_{(minor)}/MgO/Al_2O_3$, $Mo_{(major)}/M_{(minor)}/MgO/Al_2O_3$ and $Ni/Ce/ZrO_2$ catalysts were prepared for the ATR of *iso*-octane and toluene. The various catalyst formulations were prepared by the method of incipient wetness of the γ-alumina with aqueous solutions of the corresponding metal nitrates. The solution containing the metal salts was added drop wise to the pre-calcined supports until incipient wetness was reached. The materials were slowly dried at 80 °C for 6 h and then the final products were calcined at 650 °C for 5 h in an air.

$Ni/Ce/ZrO_2$ catalyst was prepared via urea hydrolysis. $Ce(NO_3)_3{\cdot}6H_2O$ and $ZrO(NO_3)_2{\cdot}xH_2O$ salts were dissolved in distilled water to the desired concentration. The proportion of metals (Ce and Zr) in solid solution was $Ce_{0.7}Zr_{0.3}O_2$. Then, the mixed metal salt solution was added to a 0.4 M of urea solution, keeping salt to urea solution ratio of 2:1 (v/v), followed by aging the mixture overnight at 100 °C. Then the solution was filtered to separate the solid part. The solid cake was washed with distilled water and dried overnight in an oven at 110 °C. Finally the product was calcined at 500 °C for 4 h. The formulations of the catalyst prepared in this work are summarized in Table 1.

2.3. ATR reaction system

The performance of the commercial and the prepared catalysts was measured in a *iso*-octane autothermal reforming system. The schematic diagram of ATR system is presented in Fig. 1. 1 g of ATR catalyst was charged in the inconel reactor and was pretreated at 700 °C for 1 h under a hydrogen flow of 60 cm^3/min. All runs were conducted in the temperature range of 550–750 °C at atmospheric pressure with a space velocity in a range 8000–10,000 h^{-1}, feed molar ratios of $H_2O/C = 3.0$ and $O/C = 1.0$. The reactant air was delivered by mass flow controller and liquid reactants; H_2O, *iso*-octane and toluene were fed by liquid delivery pumps (Young Lin Co., Model M930). The gas effluent was analyzed by on-line gas chromatograph (HP-6890 N) equipped with a TCD and a carbosphere column (0.0032 m O.D. and 3.048 m length, 80/100 meshes).

2.4. Catalyst characterization

The catalysts were characterized by N_2 physisorption, XRD, SEM and TEM techniques before and after the ATR reaction. BET surface area and total pore volume of the catalysts were determined from the N_2 adsorption isotherm measured at liquid nitrogen temperature with a sorption analyzer [Quantachrome Co., Autosorb-1C]. The active metal surface area of the catalysts was calculated by CO chemisorption at 400 °C using a CO chemisorption analyzer [Micrometrics Co., Autochem II]. The structural properties of the catalysts were determined with an X-ray diffraction (XRD) analyzer [Shimazdu Co., XRD-6000] using Cu Kα radiation produced at 40 kV and 30 mA and a scanning speed of 5°/min. Also, micro structure and morphology of catalysts were characterized by TEM [Philips Co., M30] and SEM [Hitachi Co., S-4200]. The contents of carbon and sulfur were analyzed by elemental inorganic analyzer [Lego Co., CS-344].

3. Results and discussion

3.1. Consideration for thermodynamic equilibrium

The overall ATR reaction of *iso*-octane is given by

$$C_nH_m + a(O_2 + 3.76N_2) + (2n - 2a)H_2O \rightarrow nCO_2 + (2n - 2a + m/2)H_2 + 3.76aN_2$$

where, *a* is the molar ratio of oxygen/fuel. The heat of the gross-reaction depends on the molar ratio of oxygen/fuel, the molar ratio

Table 1
The compositions of the prepared and the commercial catalysts

Catalyst code	Active component (mol%)				Basic component (mol%)		Support (mol%)	
	Ni	Fe	Co	Mo	MgO	Al_2O_3	SiO_2-Al_2O_3	Ce/ZrO_2
KIST-A	14.7	–	–	–	11.5	31.5	–	–
KIST-B	–	14.7	–	–	11.5	31.5	–	–
KIST-C	–	–	14.7	–	11.5	31.5	–	–
KIST-D	–	–	–	14.7	11.5	31.5	–	–
KIST-E	14.7	–	–	–	11.5	–	31.5	–
KIST-F	–	14.7	–	–	11.5	–	31.5	–
KIST-G	–	–	14.7	–	11.5	–	31.5	–
KIST-H	–	–	–	14.7	11.5	–	31.5	–
KIST-I	11.76	2.94	–	–	11.5	31.5	–	–
KIST-J	11.76	–	2.94	–	11.5	31.5	–	–
KIST-K	11.76	–	–	2.94	11.5	31.5	–	–
KIST-L	–	–	2.94	11.76	11.5	31.5	–	–
KIST-M	–	2.94	–	11.76	11.5	31.5	–	–
KIST-N	2.94	–	–	11.76	11.5	31.5	–	–
KIST-O	7	–	–	–	–	–	–	93
KIST-P	10	–	–	–	–	–	–	90
Commercial HT	–	–	–	–	–	–	–	–

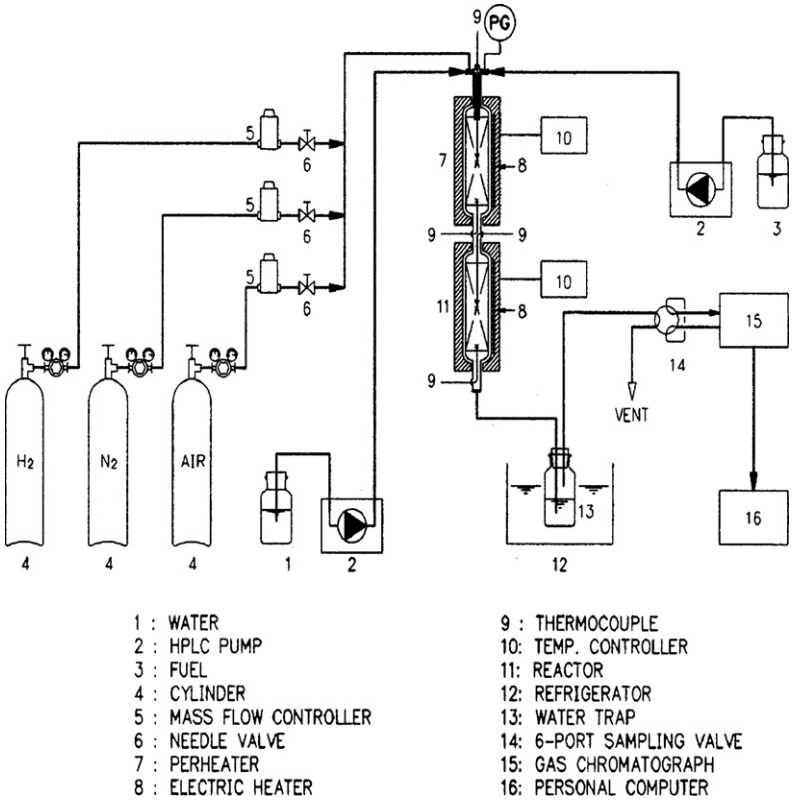

Fig. 1. A schematic diagram of *iso*-octane and toluene ATR reaction system.

of H_2O/fuel and the reaction temperature [10,11]. Generally, the reforming of hydrocarbons always has potential to form coke. If the reactor is not properly designed or operated, coking is inclined to occur. In our previous work [3–7,14], the heat of reaction for the ATR of *iso*-octane was calculated by the Gibbs free energy minimization method. It was reported [12,13] that the heat of reaction for the ATR of *iso*-octane could be properly controlled by varying the O/C and the H_2O/C molar ratio.

The reactor temperature required to prevent the formation of carbon during the reforming process of *iso*-octane was estimated by PRO-II simulation program, assuming thermodynamic equilibrium. To avoid carbon formation, the reactor temperature in the ATR of *iso*-octane can be lowered to 560 °C with molar ratio of H_2O/C = 1 and the O/C ratio = 1. The overall reaction can be shifted to the exothermic region by maintaining the O/C molar ratio higher than 0.6. The advantage of being able to tune the reaction heat by properly varying the O/C molar ratio makes ATR superior to steam reforming. Hence, when one considers the low energy requirement, an O/C molar ratio of above 0.6 is favorable for the ATR of *iso*-octane.

The amount of carbon formed as a function of temperature for five reforming reactions of *iso*-octane and toluene is presented in Fig. 2. If the feed consists of *iso*-octane (1 g mol/h) and air at O/C = 1, more than 1.e-9 μmol/h of coke would form in the partial oxidation of *iso*-octane at temperatures up to 950 °C. If the feed consists of *iso*-octane (1 g mol/h) and H_2O at H_2O/C = 1, more than 1.e-9 μmol/h of coke would occur in the steam reforming of *iso*-octane at temperatures up to 800 °C. If water is added at molar ratio of H_2O/C = 1 while maintaining the O/C ratio = 1, the reactor temperature in the POX reforming of *iso*-octane can be lowered to 560 °C before carbon formation occurs.

It was observed that the carbon formation temperature was increased until 600 °C when the ATR reaction of toluene was carried out under the same reaction conditions of *iso*-octane.

We previously reported [3–7,14] the problem of catalyst deactivation by carbon deposition and sulfur poisoning in the ATR of *iso*-octane over a commercial reforming Haldor Topsoe (HT) catalyst. In order to figure out deactivation of HT catalyst, the characteristics of the catalysts before and after the reaction were investigated by N_2 physisorption, CO chemisorption and elemental inorganic analysis.

The compositions of the prepared and the commercial HT catalysts are summarized in Table 1. The used catalysts were classified as $M_{(active)}/MgO/Al_2O_3$ (KIST-A, B, C and D), $M_{(active)}$/MgO/

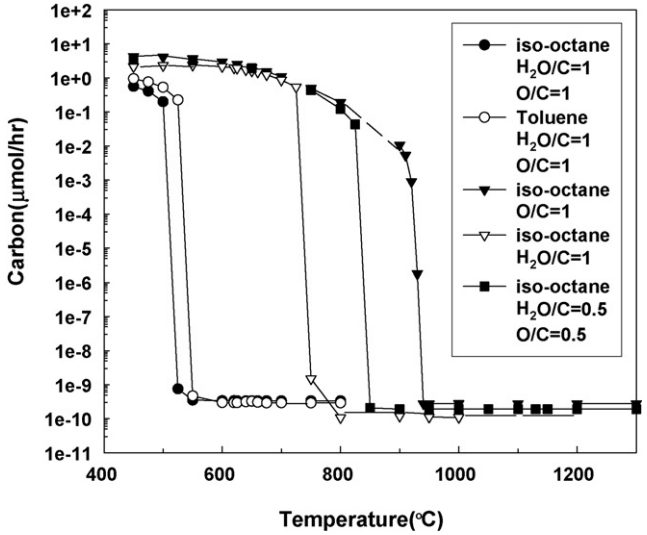

Fig. 2. Reaction temperature required to prevent the formation of carbon during the reforming process of *iso*-octane and toluene, assuming thermodynamic equilibrium.

Table 2
The characteristics of the prepared and the commercial catalysts

Catalyst code	Catalyst formulation	BET S.A. (m^2/g)	Total P.V. (cm^3/g)	Average pore D. (Å)
KIST-A	$Ni/MgO/Al_2O_3$	28.90	0.206	286.0
KIST-B	$Fe/MgO/Al_2O_3$	87.80	0.227	103.7
KIST-C	$Co/MgO/Al_2O_3$	65.74	0.305	185.6
KIST-D	$Mo/MgO/Al_2O_3$	87.74	0.294	134.1
KIST-E	$Ni/MgO/SiO_2$-Al_2O_3	84.82	0.226	165.5
KIST-F	$Fe/MgO/SiO_2$-Al_2O_3	133.6	0.310	92.90
KIST-G	$Co/MgO/SiO_2$-Al_2O_3	92.84	0.335	136.8
KIST-H	$Mo/MgO/SiO_2$-Al_2O_3	128.1	0.321	98.92
KIST-I	$Ni/Fe/MgO/Al_2O_3$	73.55	0.211	115.1
KIST-J	$Ni/Co/MgO/Al_2O_3$	61.61	0.172	111.8
KIST-K	$Ni/Mo/MgO/Al_2O_3$	72.44	0.258	124.4
KIST-L	$Mo/Co/MgO/Al_2O_3$	92.61	0.370	160.1
KIST-M	$Mo/Fe/MgO/Al_2O_3$	95.71	0.202	84.44
KIST-N	$Mo/Ni/MgO/Al_2O_3$	85.95	0.303	141.4
KIST-O	Ni/CeO_2-ZrO_2	41.52	0.099	9.55
KIST-P	Ni/CeO_2-ZrO_2	51.24	0.108	8.45
Commercial HT	$Ni/CaO/Al_2O_3$	24.92	0.154	286.5

SiO_2-Al_2O_3 (KIST-E, F, G and H), $Ni_{(major)}$-$M_{(minor)}/MgO/Al_2O_3$ (KIST-L, M and N), $Ni/CeZrO_2$ (KIST-O and P) and commercial HT catalysts. The characteristics of the prepared and the commercial HT catalyst are summarized in Table 2. BET surface area of Ni-based bimetallic catalysts supported on MgO and Al_2O_3 is higher than that of $Ni/MgO/Al_2O_3$. It was observed that BET surface area of Ni-based bimetallic catalysts was higher than $Ni/Ce/ZrO_2$ catalyst even though the amount of Ni loading of bimetallic catalyst was higher than those of $Ni/Ce/ZrO_2$ catalysts.

3.2. ATR reactions of iso-octane and toluene

The comparison of product distribution in the ATR of *iso*-octane over the prepared and commercial HT catalysts is summarized in Table 3. Many of the experimented catalyst formulations displayed reasonably good activity towards the ATR of *iso*-octane. The Fe-supported system showed better activity than the other catalyst in the general formula $M_{(active)}/MgO/Al_2O_3$. Ni supported system displayed substantially low activity. However, the large amounts of CO and CH_4 over the Fe and Co supported systems made them undesirable for ATR reactions [4,5]. In the catalyst system (KIST-A, B, C, D, E, F, G and H) with $M_{(active)}$/support, there is no correlation between H_2 selectivity and supports (Al_2O_3 and SiO_2-Al_2O_3) used. However, considering the selectivity of CH_4, $M_{(active)}/Al_2O_3$ catalyst formulation is more desirable than $M_{(active)}/SiO_2$-Al_2O_3 catalyst system.

All $M_{(active)}/MgO/Al_2O_3$ catalysts were seriously deactivated with time on stream due to the formation of carbon(not shown). To minimize the formation of carbon, Ni-based bimetallic catalysts with general formula $Ni_{(major)}M_{(minor)}MgO/Al_2O_3$, $Mo_{(major)}M_{(minor)}MgO/Al_2O_3$ and $Ni/CeZrO_2$ were prepared and tested under the same reaction conditions. It was found that the Ni-based bimetallic catalysts and $Ni/CeZrO_2$ showed higher H_2 selectivity than $M_{(active)}/MgO/Al_2O_3$ and $Mo_{(major)}M_{(minor)}MgO/Al_2O_3$ catalysts.

In the case of the systems possessing Ni as the major component, both Fe and Co were found to be very effective components, which in very small amounts can considerably enhance the performance of the Ni-based systems. The considerable enhancement in the catalytic activities of the nickel based systems doped with small amounts of promoter such as Fe and Co may be due to synergistic effect of the active components and the supports, resulting in the proper dispersion of the active components, thereby, providing more active sites for the reaction.

Fig. 3 shows the comparison of the product composition and coke deposition temperature for the ATR of *iso*-octane and toluene over KIST-I catalyst. Equilibrium conversion and carbon formation

Table 3
Comparison of product distribution for ATR reaction of *iso*-octane over the prepared and commercial H-T catalysts at 700 °C

Catalyst code	Reaction condition			Product distribution (mol%)			
	S.V. (h^{-1})	H_2O/C (molar ratio)	O/C (molar ratio)	H_2	CO	CO_2	CH_4
KIST-A	8776	3	1	46.83	43.86	3.03	6.28
KIST-B	8776	3	1	58.07	19.57	19.91	2.45
KIST-C	8776	3	1	56.22	18.95	20.69	4.13
KIST-D	8776	3	1	43.74	22.75	24.24	9.23
KIST-E	8776	3	1	60.03	18.14	15.44	6.39
KIST-F	8776	3	1	44.07	33.92	16.28	5.72
KIST-G	8776	3	1	56.20	20.82	18.44	4.54
KIST-H	8776	3	1	41.64	24.84	25.91	7.61
KIST-I	8776	3	1	62.77	12.75	22.76	1.72
KIST-J	8776	3	1	63.73	12.88	22.25	1.13
KIST-K	8776	3	1	61.18	12.96	23.28	2.58
KIST-L	8776	3	1	56.61	10.29	26.16	6.94
KIST-M	8776	3	1	40.86	31.77	17.07	10.30
KIST-N	8776	3	1	49.74	33.66	11.47	5.13
KIST-O	10,000	3	1	61.91	17.25	18.9	1.92
KIST-P	10,000	3	1	62.8	15.98	20.35	0.84
Commercial HT	8776	3	1	64.71	11.53	23.39	0.37

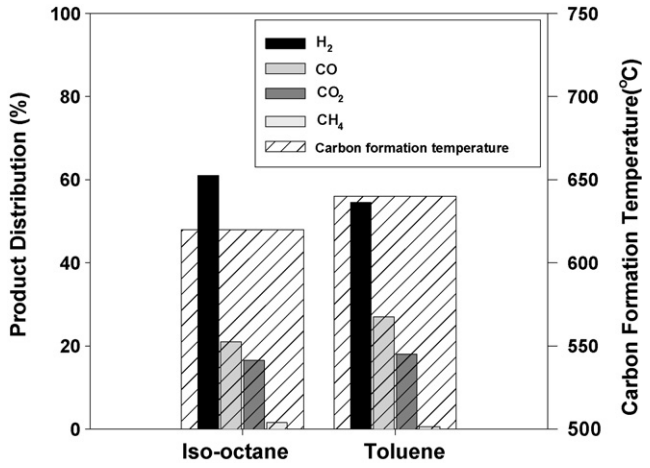

Fig. 3. The comparison of the product composition and coke deposition temperature for the ATR of *iso*-octane and toluene, respectively over KIST-I catalyst. Reaction conditions: temperature = 700 °C; feed molar ratio of $H_2O/C = 3$ and $O/C = 1$.

temperature for ATR reaction of *iso*-octane and toluene were estimated by POR II simulation program, assuming thermodynamic equilibrium at 700 °C, feed molar ratios of $H_2O/C = 3$ and $O/C = 1$.

The carbon formation in the ATR reaction of *iso*-octane occurred at less than 620 °C, however, it was also found that it occurred at less than 640 °C for toluene. The results suggest that the selection of reasonable reforming temperature is important for the reforming of mixed hydrocarbons such as gasoline because of higher reforming temperature of toluene than that of *iso*-octane. Conversions of *iso*-octane and toluene were 100% under the tested conditions.

In the case of bimetallic catalyst systems (KIST-L, M and N) possessing Mo as the major component, all catalysts showed lower H_2 selectivity than the Ni-based bimetallic catalyst system (KIST-I, J and K).

Fig. 4 shows comparison of product distribution for ATR of *iso*-octane over the KIST-I, KIST-J and commercial HT catalysts [3,4,6]. The ATR reactions were carried out at the reaction temperature of

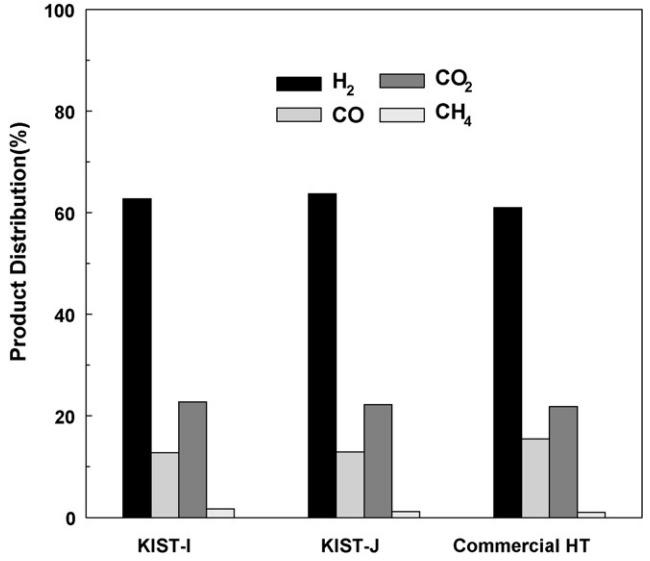

Fig. 4. Comparison of product distribution for ATR of *iso*-octane over the KIST-I, KIST-J and commercial HT catalysts. Reaction temperature = 700 °C; space velocity = 8776 h^{-1}; feed molar ratio of $H_2O/C = 3$ and $O/C = 1$.

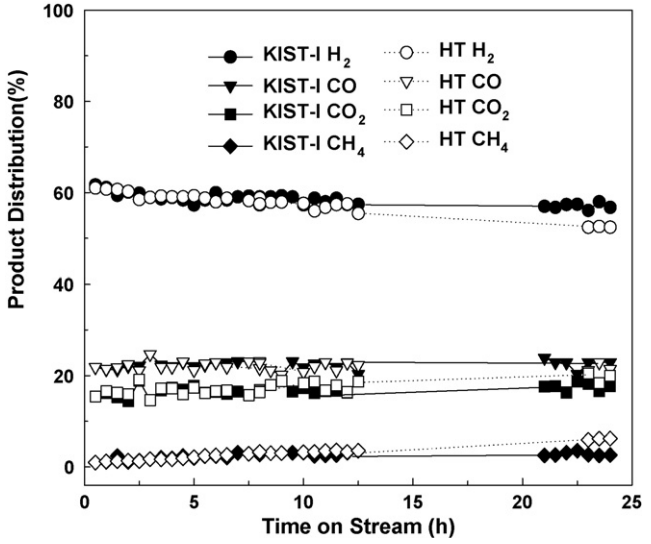

Fig. 5. Sulfur tolerance for the KIST-I and commercial HT catalysts in the ATR reaction of *iso*-octane containing 100 ppm of sulfur. Reaction temperature = 700 °C; space velocity = 8776 h^{-1}; feed molar ratio of $H_2O/C = 3$ and $O/C = 1$.

700 °C with a space velocity of 8776 h^{-1}, feed molar ratios of $H_2O/C = 3$ and $O/C = 1$.

The formulations based on Ni as the major active component and Fe or Co as the minor component are promising systems with comparable activity or even superior to the commercial systems. However, KIST-I catalyst showed slightly higher stability for carbon formation than KIST-J catalyst in ATR of *iso*-octane (not shown). Therefore, KIST-I catalyst was selected as the best candidate catalyst for ATR of *iso*-octane under the tested reaction conditions.

In our previous work [3–6,13], some KIST catalysts showed better activity and sulfur tolerance than the commercial HT catalyst in the ATR of *iso*-octane containing of 5 ppm sulfur. Fig. 5 shows the comparison of the KIST-I with the commercial HT catalyst for sulfur tolerance in the ATR *iso*-octane containing 100 ppm of sulfur. The KIST-I catalyst displayed better sulfur

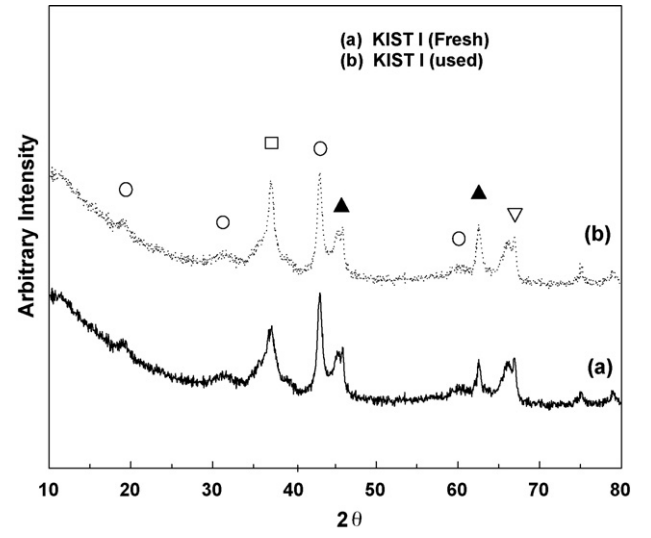

Fig. 6. The XRD patterns of the KIST-I catalysts before and after the ATR reaction of *iso*-octane (containing 100 ppm sulfur) for 24 h (○) NiO, (▲) $MgAl_2O_4$, (□) $FeAl_2O_4$, (▽) Ni.

Table 4
Characteristics of the HT and KIST-I catalysts before and after the ATR of *iso*-octane containing 100 ppm sulfur for 24 h

Catalyst		BET S.A.[a] (m^2/g)	Total P.V.[a] (cm^3/g)	Active M. S.A.[b] (m^2/g)	Carbon content[c] (wt.%)	Sulfur content[c] (wt.%)
HT	Before reaction	24.92	0.1541	0.5043	0.098	0.003
	After reaction	16.34	0.1749	0.1999	24.0	0.00
KIST I	Before reaction	73.55	*0.212*	*1.906*	0.098	0.003
	After reaction	49.38	0.166	1.397	19.6	0.005

[a] Derived from N_2 adsorption.
[b] Derived from CO chemisorption.
[c] Analyzed by elemental inorganic analyzer.

tolerance than the commercial HT catalyst. There is no major change in structure of catalyst as shown in Fig. 6.

The characteristics of catalysts after the ATR reaction of *iso*-octane containing 100 ppm sulfur for 24 h are summarized in Table 4. The BET surface area of KIST-I and commercial HT catalysts decreased by 32.9% and 34.5% respectively after the ATR reaction whereas active metal surface area of these catalysts decreased by 26.7% and 60.4% respectively after the reaction. Even though KIST-I catalyst is more sulfur tolerant than the HT catalyst, a new high performance coke- and sulfur-resistant catalyst needs to be developed for applying in the ATR reactor based on gasoline feed. The results revealed that the carbon deposition on surface of the catalyst was accelerated by increasing sulfur content in *iso*-octane. However, there was no accumulation of sulfur in catalysts after the reaction of *iso*-octane containing 100 ppm sulfur.

Fig. 7 shows the long-term catalytic stability for KIST-I catalyst in the ATR reaction of *iso*-octane containing sulfur of less than 5 ppm at 700 °C with a space velocity of 8778 h^{-1} and feed molar ratio of $H_2O/C = 3$ and $O/C = 1$ for 760 h. It was observed that there was no major change in the product distribution for ATR reaction of *iso*-octane over KIST-I and commercial HT catalysts during the time period investigated.

SEM images (Fig. 8) of KIST-I catalysts before (a) and after (b) the ATR of *iso*-octane for 760 h. It showed a little carbon deposition on the surface of the catalyst. However, particle growth and surface destruction was not detected.

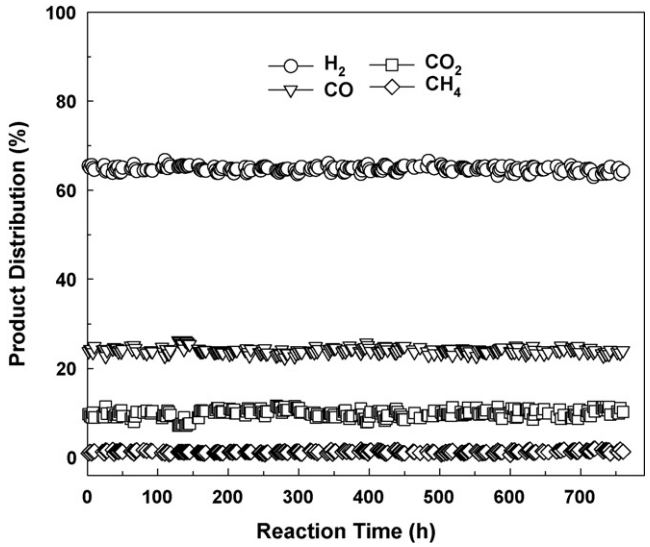

Fig. 7. Long-term stability for the KIST-I catalyst in the ATR reaction of *iso*-octane containing sulfur of less than 5 ppm [5]. Reaction temperature = 700 °C; space velocity = 8776 h^{-1}; feed molar ratio of $H_2O/C = 3$ and $O/C = 1$.

TEM micrographs of KIST-I catalyst before (a) and after (b) the ATR reaction of *iso*-octane containing sulfur less than 5 ppm at 700 °C for 760 h are shown in Fig. 9. There was no major change in the particle size of the active metal was observed. The overall results prove the higher catalytic activity of KIST-I catalyst over the commercial HT catalyst under the tested conditions.

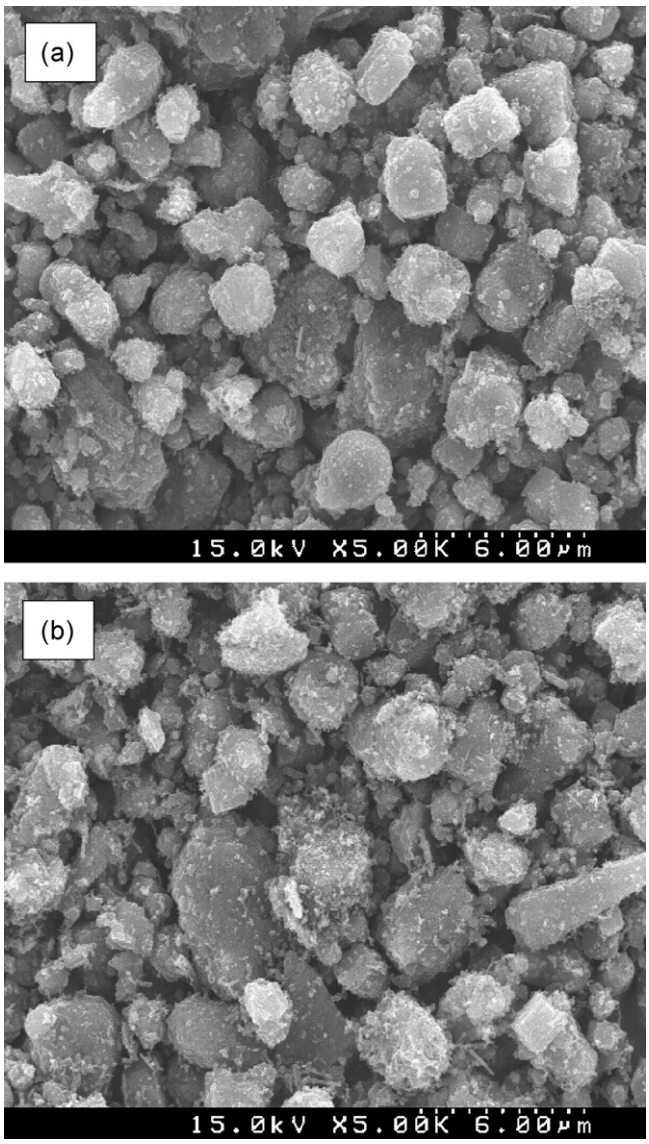

Fig. 8. SEM images of KIST-I catalysts (a) before and (b) after the ATR reaction of *iso*-octane. Reaction temperature = 700 °C; space velocity = 8776 h^{-1}; feed molar ratio of $H_2O/C = 3$ and $O/C = 1$.

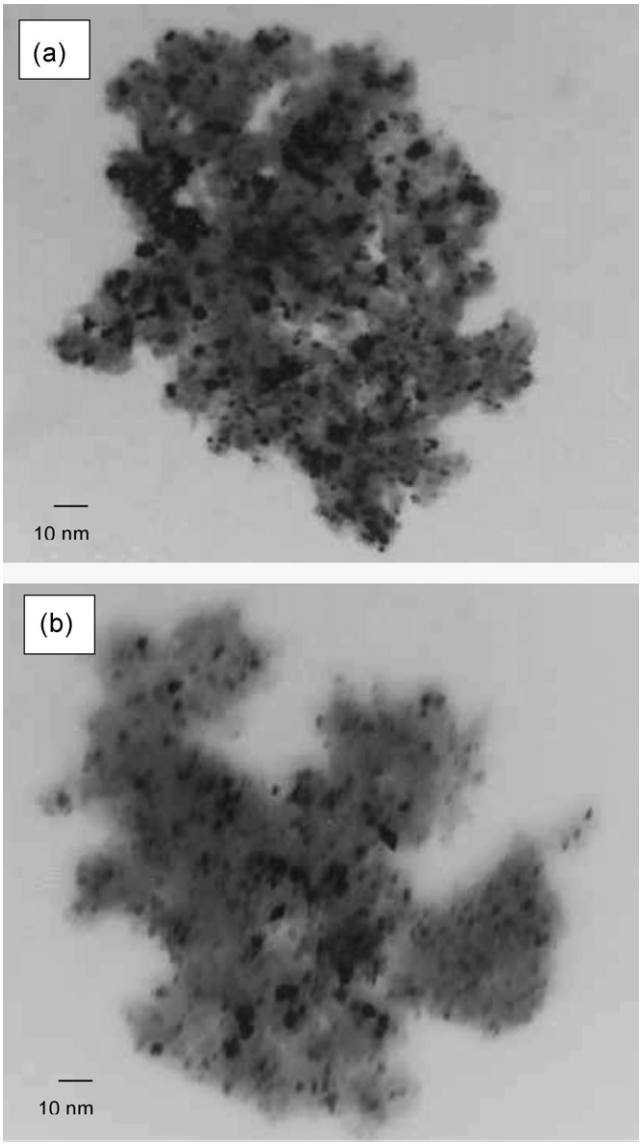

Fig. 9. TEM images of KIST-I catalysts (a) before and (b) after the ATR of *iso*-octane. Reaction temperature = 700 °C; space velocity = 8776 h^{-1}; feed molar ratio of H_2O/C = 3 and O/C = 1.

4. Conclusions

The Ni-based bimetallic catalysts displayed reasonably good activity than the other catalysts. KIST-I ($Ni/Fe/MgO/Al_2O_3$) catalyst showed better activity and sulfur tolerance over the commercial HT catalyst in the ATR reaction of *iso*-octane at 700 °C for 760 h, even though none of the systems were found to be completely sulfur tolerant. The results suggest that the $Ni/Fe/MgO/Al_2O_3$ catalyst can be applied as ATR catalyst of gasoline for fuel processor and hydrogen station systems.

Acknowledgments

This paper was performed for the development of Hydrogen Station and Fuel Reformer. We would like to thank the KIST for funding this research.

References

[1] Wenliang Zhu, Wei Han, Guoxing Xiong, Weishen yang, Catal. Today 118 (2006) 39.
[2] J.M. Ogden, T.G. Kreutz, J. Power sources 79 (1999) 143.
[3] D.J. Moon, K. Sreekumar, S.D. Lee, B.G. Lee, H.S. Kim, Appl. Catal. A 215 (2001) 1.
[4] D.J. Moon, J.W. Ryu, Catal. Lett. 89 3-4 (2003) 207.
[5] D.J. Moon, J.W. Ryu, D.M. Kang, B.G. Lee, S.D. Lee, B.S. Ahn, Korea Patent No. 10-0512911, 2005.
[6] D.J. Moon, J.W. Ryu, D.M. Kang, B.G. Lee, S.D. Lee, B.S. Ahn, USP No. US 2005/0090392, 2005.
[7] D.J. Moon, J.W. Ryu, S.D. Lee, B.G. Lee, B.S. Ahn, Appl. Catal. A 272 (2004) 53.
[8] S. Penghpanich, V. Meeyoo, T. Rirksomboon, Catal. Today 95 (2004) 93.
[9] Xiulan Cai, Xinfa Dong, Weiming Lin, J. Nat. Gas Chem. 15 (2006) 122.
[10] E.S. Putna, T. Bunluesin, X.L. Fan, R.J. Gorte, J.M. Vohs, R.E. Lakis, T. Egami, Catal. Today 50 (1999) 343.
[11] T. Takeguchi, S. F'urukawa, M. Inoue, J. Catal. 202 (2001) 14.
[12] A. Docter, A. Lamn, J. Power Source 84 (1999) 194.
[13] S.G. Chalk, J. Milliken, J.F. Miller, S.R. Venkateswaran, J. Power Source 71 (1998) 26.
[14] Development of Multi-Fuel Processor for Fuel Cell Vehicle, KIST report UCE 1702(2)-7118-6, 2001.